

Copyright Warning & Restrictions

The copyright law of the United States (Title 17, United States Code) governs the making of photocopies or other reproductions of copyrighted material.

Under certain conditions specified in the law, libraries and archives are authorized to furnish a photocopy or other reproduction. One of these specified conditions is that the photocopy or reproduction is not to be “used for any purpose other than private study, scholarship, or research.” If a user makes a request for, or later uses, a photocopy or reproduction for purposes in excess of “fair use” that user may be liable for copyright infringement,

This institution reserves the right to refuse to accept a copying order if, in its judgment, fulfillment of the order would involve violation of copyright law.

Please Note: The author retains the copyright while the New Jersey Institute of Technology reserves the right to distribute this thesis or dissertation

Printing note: If you do not wish to print this page, then select “Pages from: first page # to: last page #” on the print dialog screen

The Van Houten library has removed some of the personal information and all signatures from the approval page and biographical sketches of theses and dissertations in order to protect the identity of NJIT graduates and faculty.

THE STUDY ON THE SOOT FORMATION
OF HYDROCARBON FLAMES

BY

YIH-JIAN WU

A THESIS

PRESENTED IN PARTIAL FULFILLMENT OF

THE REQUIREMENTS FOR THE DEGREE

OF

MASTER OF SCIENCE IN CHEMICAL ENGINEERING

AT

NEWARK COLLEGE OF ENGINEERING

This thesis is to be used only with due regard to the rights of the author(s). Bibliographical references may be noted, but passages must not be copied without permission of the College and without credit being given in subsequent written or published work.

Newark, New Jersey
1974

ABSTRACT

Carbon formation during the quenching of low-pressure premixed hydrocarbon flames was studied using rapid-scanning optical and mass spectroscopy. Experimental techniques were developed and it was found that the tendency to form soot was a function of the hydrocarbon chain length. These results are relevant to the design of restartable space engines in which the use of hydrocarbon fuels is contemplated because the formation of soot in space will result in the formation of a shroud around the spacecraft which will adversely affect sensing by optical means.

APPROVAL OF THESIS

THE STUDY ON THE SOOT FORMATION
OF HYDROCARBON FLAMES

BY

YIH-JIAN WU

DEPARTMENT OF CHEMICAL ENGINEERING
NEWARK COLLEGE OF ENGINEERING

BY

FACULTY COMMITTEE

APPROVED: _____

NEWARK, NEW JERSEY

JUNE, 1974

ACKNOWLEDGEMENTS

I would like to express my sincere gratitude to Dr. Leonard Dauerman for his kind advice and guidance in the preparation of this thesis.

My thanks goes to NASA for the grant which financed this research.

TABLE OF CONTENTS

	<u>PAGE</u>
Title Page	i
Abstract	ii
Approvals	iii
Acknowledgements	iv
Table of Contents	v
List of Figures	vi
Introduction	1
Experimental	5
Apparatus and Experimental Procedure	5
1. Burner	5
2. Spectrometer and Auxiliary Equipment	5
3. Mass Spectrometer	7
4. Temperature of Flame	7
5. Characteristics of Burners	8
Results and Discussion	11
Conclusions	15
References	30

LIST OF FIGURES

	<u>PAGE</u>
Figure 1 System Used to Study Spectra of Quenched Flames	17
Figure 2 Rotameter Calibrated with Wet Test Meter	18
Figure 3 IR Spectra Before Quenching (on the left) and After Quenching; Absorption and Emission Spectra are Displayed	19
Figure 4 UV-Visible Spectra of Quenched Flame	20
Figure 5 Steady-State IR Spectra of Sooty vs Non-Sooty Flames	21
Figure 6 Composition of Flame From IR Spectra During Quenching of 1:1 CH ₄ to O ₂ vs Time	22
Figure 7 Composition of Flame From IR Spectra During Quenching of 1:2.5 Butane to O ₂ vs Time	23
Figure 8 Composition of Flame From UV-Visible Spectra During Quenching of 1:2.5 Butane to O ₂ vs Time	24
Figure 9 Steady-State UV-Visible Spectra of Methane/Oxygen Flame in Various Concentrations	25

LIST OF FIGURES

	<u>PAGE</u>
Figure 10 Steady-State UV-Visible Spectra of Butane/Oxygen Flame in Various Concentrations	26
Figure 11 Steady-State Mass Spectra Data of Non-Sooty Flame	27
Figure 12 Steady-State Mass Spectra Data of Sooty Flame	28
Figure 13 Flame Velocity of Burner System	29

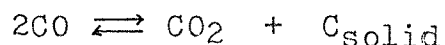
INTRODUCTION

In a reaction control engine, a problem which has to be avoided is the emission of soot particles. It is thought that such particles will be deleterious because they will be expected to act like a shroud around the spacecraft and, thereby, affect optical sighting and, also, may have an effect upon instrumentation performance.

Methane, recovered from carbon dioxide by the Sabatier-Senderens reaction, could be used as a fuel in a rocket engine without the formation of soot in the exhaust product, as suggested by Levine¹. In the performance of a rocket engine, it is of interest to characterize the factors which affect the formation of soot. It has been established that to suppress soot formation the amount of oxygen needed is above that calculated thermodynamically. The formation of soot is a kinetically controlled process. The work of Homann² on pre-mixed flames and the work of Mentrop³ on turbulent diffusion flames indicate that the kinetically-controlled process for the formation of soot involves not only slow chemical reactions, but perhaps, even more significantly, an unmixing effect. Reactions are diluted by hot product gases before the reaction occurs. It is also possible that reactive species in the recirculating gas promote pyrolysis. Hydrocarbon pyrolysis occurs in a non-oxidizing atmosphere and

the soot particles formed oxidize slowly in an oxidizing atmosphere.

An experiment carried out in this study is suggestive of the results to be expected in space engines. Since these are restartable engines, the formation of soot is most likely to occur during start-up and shut-down because during these stages the fuel to air or oxygen ratios fluctuate over a wide range and, also, the combustion temperature drops. This temperature drop favors the formation of soot thermodynamically because the equilibrium



is well over to the right below 1000° K and, also, the rate of combustion decreases. (14)

Most of the experimental results for the formation of carbon soot in premixed hydrocarbon-air or hydrocarbon-oxygen flames have been obtained with flames at atmospheric pressure. Measurements of the onset of carbon formation in Bunsen burner flames have been made by Street & Thomas⁴. The critical O/C ratio at which carbon formation starts which is characterized by the beginning of the yellow luminosity in the burned gases was studied for various fuels. In most cases carbon luminosity occurs for mixtures which are much less rich in fuel than those required to liberate free carbon under equilibrium conditions. Only for acetylene

is the observed luminosity point anywhere near that expected for equilibrium. Several authors⁵⁻⁸ have described attempts to collect data for the explanation of the mechanism of carbon formation. The present state of our knowledge including various theoretical interpretations are summarized in the books of Gaydon and Wolfhard⁹ and of Minkoff and Tipper,¹⁰ and the article of Street and Thomas⁴ and, recently, Homann and Wagner.¹⁵

Measurements under atmospheric pressure have shown that it is rather hard to resolve the concentration distribution of intermediates which are supposed to be important for carbon formation. Bonne, Homann and Wagner¹¹ studied the formation of carbon in pre-mixed flame at reduced pressure. Reduction of pressure increases the length of the main reaction zone of the flame and that of the zone of particle growth as well. At pressure between 0.1 atm and 0.25 atm, the length of the zone in which carbon formation takes place is the order of 1 cm. They have shown that in order to understand the nature of soot formation in flames, it is necessary to probe the flame using both mass spectrometry and optical spectrometry.

The purpose of this study was to determine whether or not the sudden quenching of combustion caused by a drop in the oxygen flow rate, even at very low chamber pressure, will lead to soot formation and, also, the transient phenomena of the flame simulated in the engine start-up and shut-down.

It was our ultimate aim to study on unstable flame using simultaneously rapid-scanning optical and mass spectrometry. It was hoped that an investigation of soot formation in an unstable system might lead to criteria for deciding whether or not a process in a stable flame is kinetically or thermodynamically stabilized.

EXPERIMENTAL

Apparatus and Experimental Procedure

1. Burner: A premixed flat flame burner with a water cooled 2 cm diameter x 3 mm thick sintered bronze plate for stabilization of the flame was used in the experiment. The burner was enclosed in a 1 1/2 inch x 1 1/2 inch pyrex pipe-cross as a burner housing to operate in low pressure atmosphere and the mixed gas was ignited with Tesla coil. The fuel and oxygen gases were metered through rotameter using Moore Flow controllers for regulation. The rotameter were calibrated using calibrated wet test meters.

2. Spectrometer and Auxiliary Equipment: The Warner & Swasey Model 501 Rapid Scanning Spectrometer was used to measure transient emission and absorption spectra of the flame; the temperature was also observed. Quenching of the flame was initiated by interrupting the flow of oxygen. This was performed by a foot actuated solenoid valve which, also, actuated a small indication light located on the top corner of the oscilloscope screen on which the time-resolved spectra were recorded.

The spectra displayed on the oscilloscope were either recorded on polaroid film or on motion picture film using a Bolex 16mm camera. The Warner & Swasey Model 501 Rapid Scanning

Spectrometer is a single beam instrument that can be operated in the infrared and the UV-visible spectral regions. While it is possible to scan limited regions of the spectra up to 1 msec. for practical reasons, the fastest scan rate in this study was 10 msec..

In this study, the IR spectra of the fuel/oxygen system was in the 2.57-4.7 μ range. N₂(liquid)-cooled InSb IR detector was used with 0.2-mm slits and 11.58-line/mm grating. In Figure 3, the IR spectra of the butane/oxygen system are shown. Two spectra are displayed simultaneously in each flame. The upper is the absorption spectrum and the lower one is the emission spectrum. A chopper was placed between absorption source lamp and flame and chopped at a rate of 10 cps. The film speed was 32 frames per second. The left hand series represent the steady-state spectra. On the right, oxygen flow has been quenched and spectra, reading downward, represent the process of quenching. In the spectra on the right note the smudge in the left hand corner. This is the light bulb signal actuated by the foot switch which causes the oxygen flow to stop. The UV spectra is in the region from .25 to .46 μ and .43 to .65 μ , a 258-line/mm grating and two photomultipliers(IP28 and 4473) were used at a slit width of 0.5 mm. In Figure 4, UV spectra in the region from .28 μ to .40 μ are shown during the quenching process. the

output from the thermocouple, which is an index of the temperature, is recorded on each frame as a straight line. The height of this line is proportional to the temperature.

Within these perimeters, species that could be detected were the following: in the IR, CO, CO₂, H₂O, hydrocarbon; in the UV-Visible, OH, CH, C₂ (Swan bands).

3. Mass Spectrometer: The Finnigan 1015 quadrupole mass spectrometer was used to analyze combustion gases which were continuously sampled by a quartz probe placed in the flame. Figure 11 shows the mass spectra data of non-sooty flame and Figure 12 shows the data of sooty flame. In the sooty flame, the acetylene peak on m/e at 26 is present and the hydrogen peak also increases.

4. Temperature of Flame: Several methods were attempted to measure the temperature of the flame. The temperature record of the flame was taken in runs separate from the analytical runs to avoid too much disturbance of the flame. Although many workers have used Pt-Pt, 10% Rh thermocouple and other devices to obtain temperatures, we found that the temperature of our flame was such that all of these devices melted in our flame.

We had available, wire for a Tungsten 5% Rhenium vs Tungsten 26% Rhenium thermocouple and found that in our flame, the rate of oxidation was slow enough to allow the

use of one thermocouple for a complete run. The Tungsten thermocouple was not catalytic to the flame gases. This was checked by coating a thermocouple with silica. The thermocouple was connected to the combination of galvanometer and oscilloscope which can detect the temperature change to 1 mv/division. The temperature measured was in the range from 2000°F to 3500°F . The temperature were also checked with pyrometer and sodium line reversal method¹³. The measurement system is illustrated schematically in Figure 1.

5. Characteristic of Burners: The flame velocity is the most important character of the burner and can be obtained from the following measurements.

1) The total amount of heat carried away by the cooling water: Q expressed in cal/ml fuel, where the volume of fuel is measured at 16°C and atmospheric pressure.

2) The mixture ratio q expressed as volume of fuel in unit volume of fuel/oxygen mixture.

3) The total volume flow rate of fuel/oxygen mixture in ml/sec: V_u -velocity of unburned mixture and laminar adiabatic flame speed S_u can be plotted against mixture ratio in the Figure 13.

Experimental Data

<u>Exp. No.</u>	<u>1</u>	<u>2</u>	<u>3</u>
O ₂ cc/sec	17.0	24.5	28.5
CH ₄ cc/sec	16.2	23.4	27.17
Flame Temp. °C	1483.7	1662.7	1628.6
Water Flow ml/sec	1.5	1.67	2.57
Cooling Water °C	8.83	8.83	5.0
Q cal/ml CH ₄	0.8179	0.6303	0.4729
O ₂ -CH ₄ Volume cc/sec	33.2	47.9	55.7

Porous disk of our burner is 2cm in diameter. Extrapolated to Q=0 get the adiabatic flame speed $S_u = 85 \text{ cc/sec} = 27.1 \text{ cm/sec}$.

A rough estimate for flame front thickness can be obtained from the equation¹³

$$L = \frac{2.5}{PV_0}$$

Where

L: Flame front thickness, cm

P: Pressure, atm.

V₀: Flame velocity, cm/sec

$$L = \frac{2.5}{\frac{100}{760} \times 27.1} = 0.7 \text{ cm}$$

The pumping capacity required for the system is

$$S = \pi r^2 v_0 = 3.14 \times 1^2 \times 27.1 = 85 \text{ cm}^3/\text{sec}$$

Where r = burner radius

RESULTS AND DISCUSSION

From the analysis of the mass spectrometric data of the combustion gases, it was observed that the richer the flame, the higher the acetylene peak. The formation of acetylene was thus used to indicate the presence of soot in the flame. The emission band associated with acetylene was also observed under steady-state conditions as the flame became sooty in the IR spectra of the rapid scanning spectrometer. In Figure 5, note that in going from the lean flame, No.2, to the richer flames, No.1,3, an emission band at 2.7μ shifted to 3.05μ . The emission band at 3.05μ can be assigned as the C-H stretch emission band of the acetylene in the IR because the other hydrocarbon C-H stretch emissors occurred at significantly higher wavelengths: Olefins at 3.2μ and aliphatics at 3.35μ . The visual observations also support the inference from the spectra that the emergence of the acetylene emission band indicated the formation of soot because the color of the leanest flame was blue while the richer flame became yellow luminosity.

Coincident with the emergency of the acetylene emission band, the O-H stretch band at 2.7μ associated with water disappeared. It is not clear at this point whether the concentration of H_2O emitters falls below the limits of

detection in sooty flames or the soot absorbed the water. That similar species can be absorbed on soot in sooty flames has been inferred previously in a study of propellant flames in the IR region¹⁶.

The observed changes in the relative intensities of the IR emission bands characteristic of CO₂ at 4.38 μ , CO at 4.86 μ and H₂O at 2.7 μ as a function of the time after quenching are plotted in Figure 6. It can be seen that the CO₂ intensity decreased at the greatest rate. It is not surprising that as less oxygen is available for combustion, CO should become the favored product. Note that those are emission spectra. The relative intensities may not reflect precisely the gas composition because at the flame temperature drops, the relative emissions may not drop proportionately.

The longer chain hydrocarbon, butane, was used to observe sooting on quenching. In this system, non-sooting combustion was sustained in the pressure region between 110 and 125 mm Hg and for a molar ratio of butane to oxygen of 1:2.5. The emission peak at 3.05 μ , which was assigned to soot, was observed on quenching by the shut off the oxygen flow of butane/oxygen flame. The flame temperature dropped 200^oF from 3100^oF to 2900^oF as the 2.7 μ peak shifted to 3.05 μ . This occurred in about 1/16 second. When this occurred, the

OH, CH, and C_2 emission bands in the UV disappeared.

The data obtained on CO, CO_2 , and H_2O in the infrared region were plotted in Figure 7. The UV-visible data were plotted in Figure 8 for C_2 , CH and OH.

The UV-visible spectra of the rich and lean flames under steady-state condition also indicated that the intensity of the C_2 emission bands decreased while the flame became leaner. In Figure 9, 10, the spectra of the rich flame, No. 1, in going to the leaner flames, No. 2, 3, shows that the emission bands of C_2 at 4737 \AA and 5165 \AA decreased their intensities while the flame became leaner.

In the methane/oxygen system, the minimum pressure at which it was possible to sustain non-sooting combustion with a 1:1 molar composition in the system used was mm Hg. The flow rate of each gas was 22 cc/sec. Under these conditions, during quenching brought about by the abrupt stopping of the oxygen flow, no emission band appeared at 3.05μ , therefore, it was inferred that soot formation did not occur.

The methanol/oxygen flame was reported to have no soot formation. In our system, the pressure of the combustion chamber was 50 mm Hg. The molar ratio of methanol/oxygen was 1:1 and the flow rate of each gas was 13 cc/sec. the

emission spectra in UV-visible region showed strong OH band on 3130.57 \AA and the moderate intensity of CH band on 4298.71 \AA but no indication of C_2 band. The major bands in the IR emission spectra were H_2O at 2.7μ and CO_2 at 4.3μ , no emission band appeared at 3.5μ . The mass spectra of methanol/oxygen flame also showed no indication of C_2 products.

CONCLUSIONS

Jost, Wagner and Homann have shown that in order to understand the nature of soot formation in flames, it is necessary to probe the flame using both mass spectrometry and optical spectrometry. One of their major conclusions was that the back-diffusion of hydrogen causes "Unmixing" of premixed flames. This mechanism explains why soot is formed from a stoichiometric mixture which theoretically should not produce a sooty flame.

Many combustion systems are unstable. Unfortunately in our present sample probing system of the mass spectrometer, it is very difficult to detect the change of the transient phenomena of the flame because the sample passage to the mass spectrometer is long and can not respond to the change quick enough. But in the steady-state flame, both optical and mass spectrometer can detect the presence of acetylene on the formation of the soot. In the hydrocarbon/oxygen system, the longer the chain the easier the formation of the soot. In aliphatic hydrocarbon flames, acetylene can be a measurement of the expected degree of soot formation.

In the methane/oxygen system, non-sooty combustion can be maintained at extremely low pressures, and that the quenching of such a system will not cause soot formation. The

probability is that proper conditions for shut down can be achieved without soot formation being a problem.

Figure 1 System Used to Study Spectra of Quenched Flames

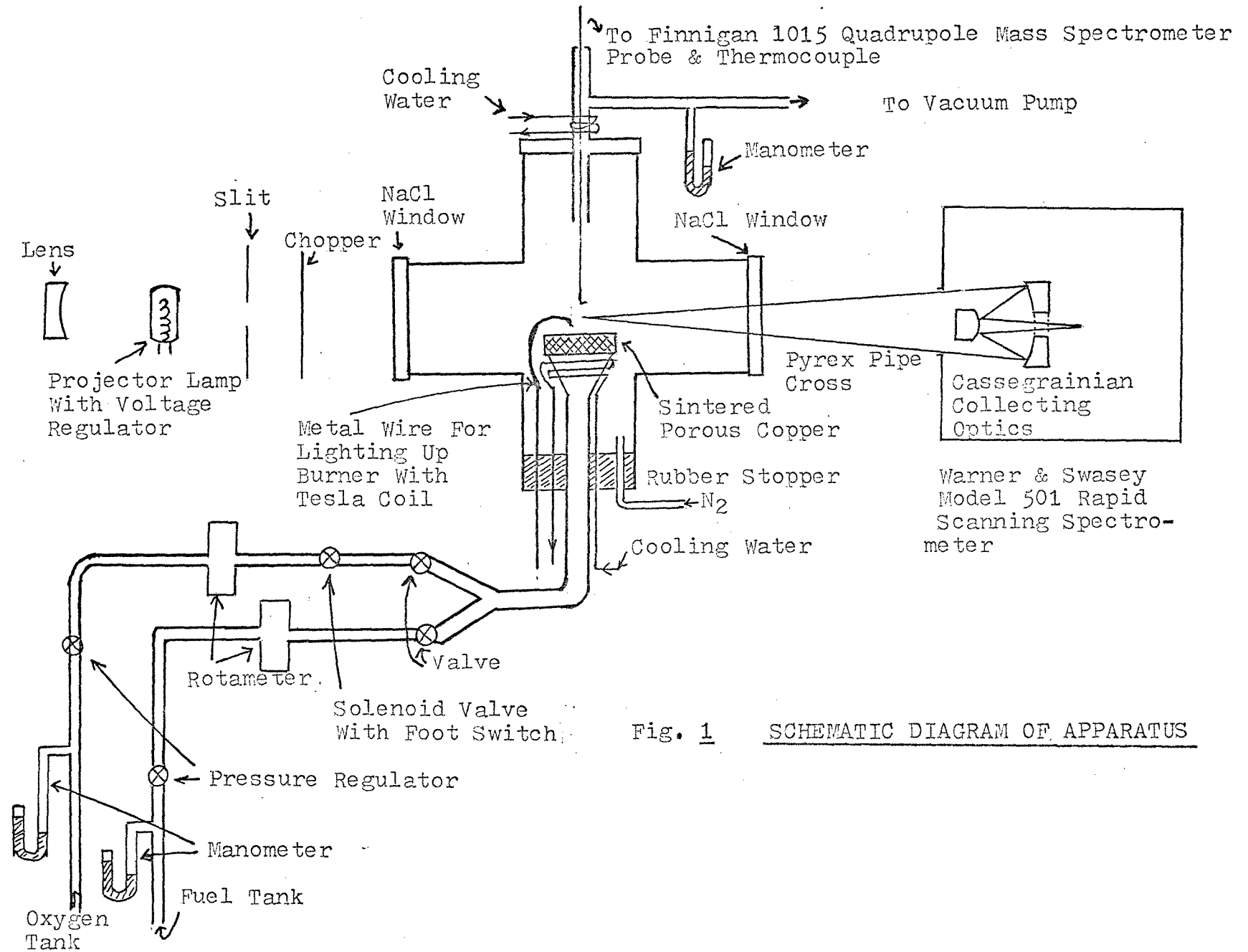


Fig. 1 SCHEMATIC DIAGRAM OF APPARATUS

Figure 2 Rotameter Calibrated with Wet Test Meter

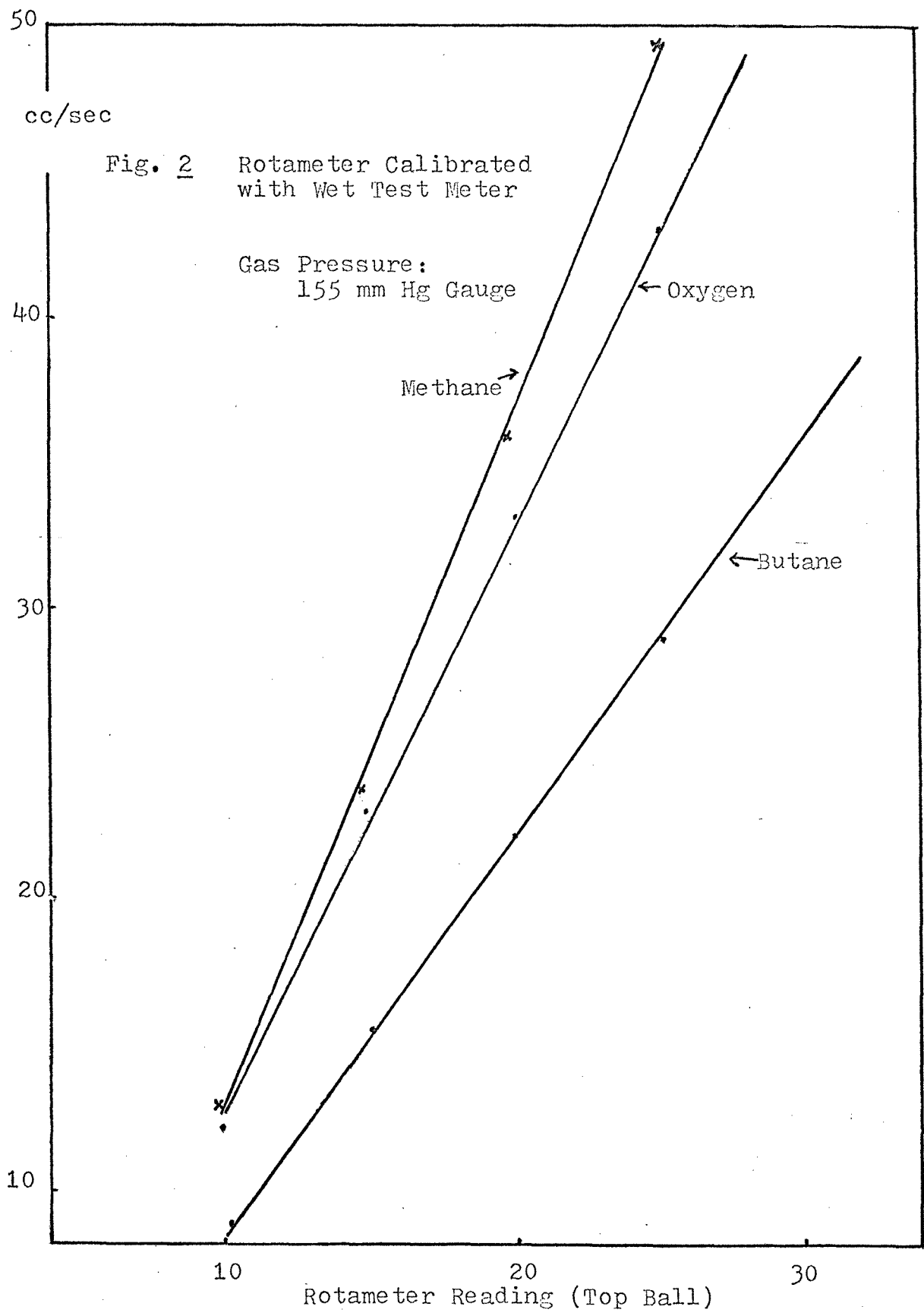


Figure 3 IR Spectra Before Quenching (on the left) and After Quenching; Absorption and Emission are Displayed

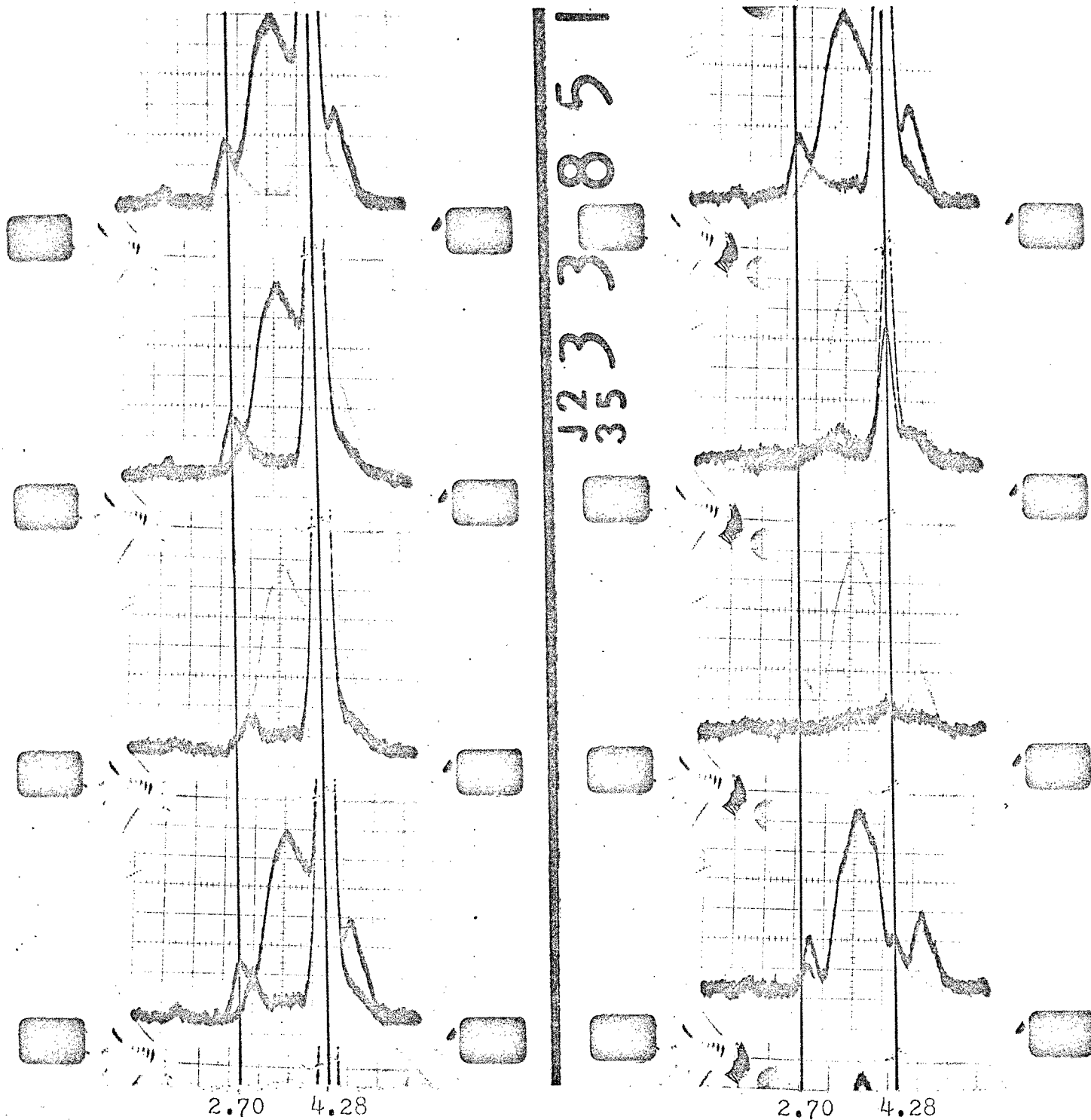


Fig. 3 IR Spectra Before Quenching(on the left) and After Quenching: Absorption and Emission Spectra are Displayed
 Butane: 11 cc/sec, Oxygen: 28.5 cc/sec
 Pressure: 100 mm Hg

Figure 4 UV-Visible Spectra of Quenched Flame

Fig. 4 UV-Visible
Spectra of Quenched
Flame

Methane 21.8 cc/sec
Oxygen 22.5 cc/sec
Pressure 65 mm Hg

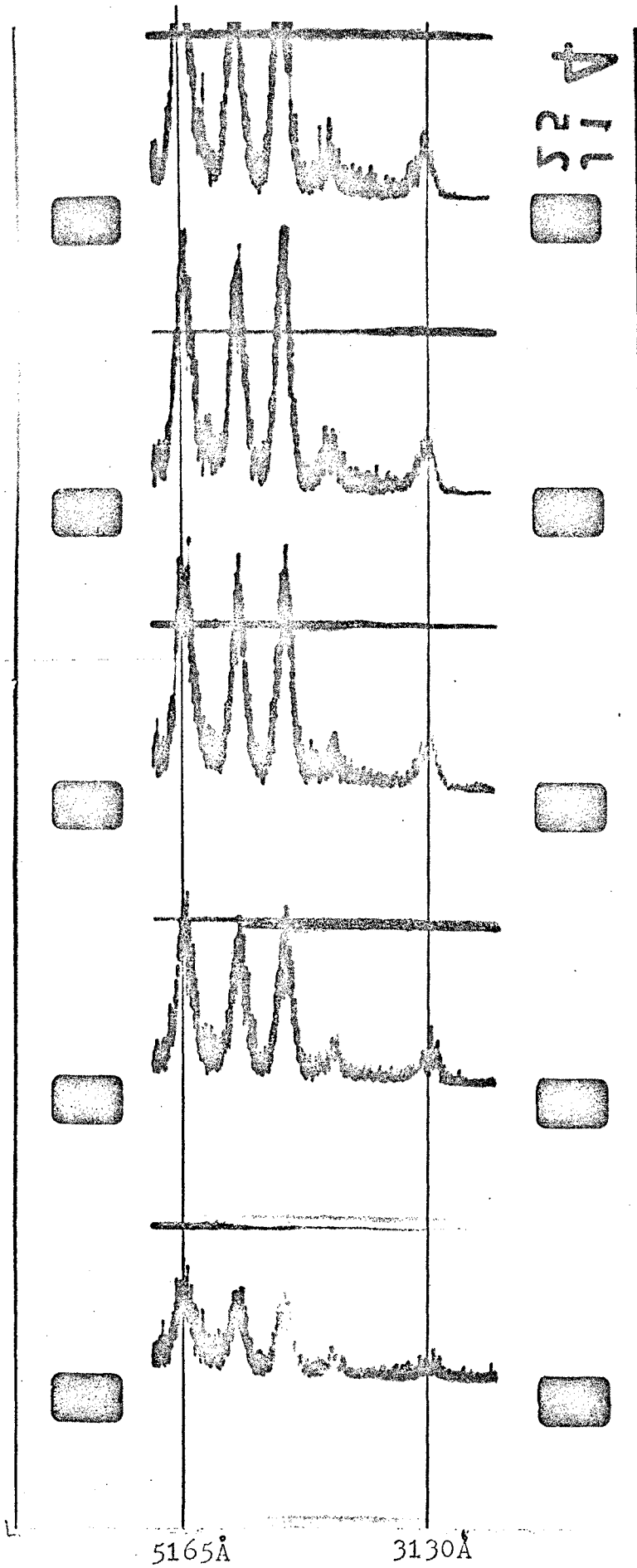


Figure 5 Steady-State IR Spectra of Sooty vs Non-Sooty Flames

Fig. 5 Steady-State
IR Spectra of Sooty v.
Non-Sooty Flames

No. 1

richer flame

No. 2

lean flame

No. 3

richest flame

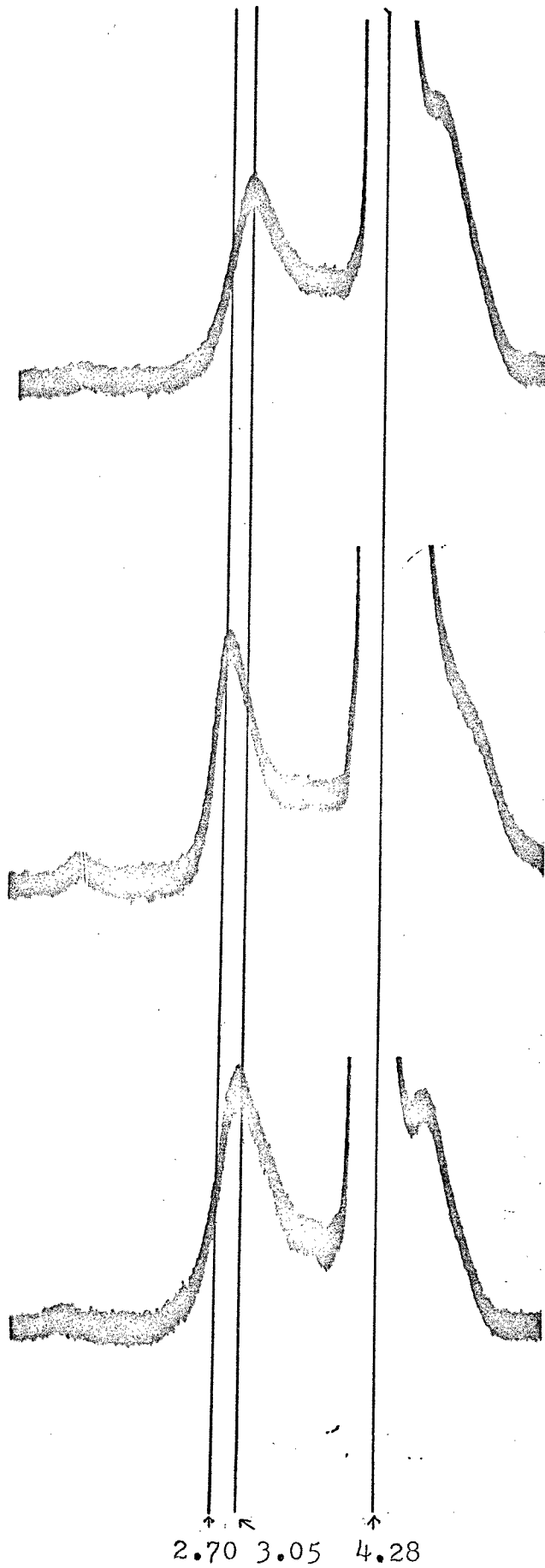


Figure 6 Composition of Flame From IR Spectra During
Quenching of 1:1 CH₄ to O₂ vs Time

Intensity
(Relative Peak
Height)

Fig. 6 Fuel Mixture: 1:1 (molar)
Methane to Oxygen
Pressure: 70 mm Hg
Data taken from 6 different runs:
Infrared Spectra

x : CO₂
Δ : CO
o : H₂O

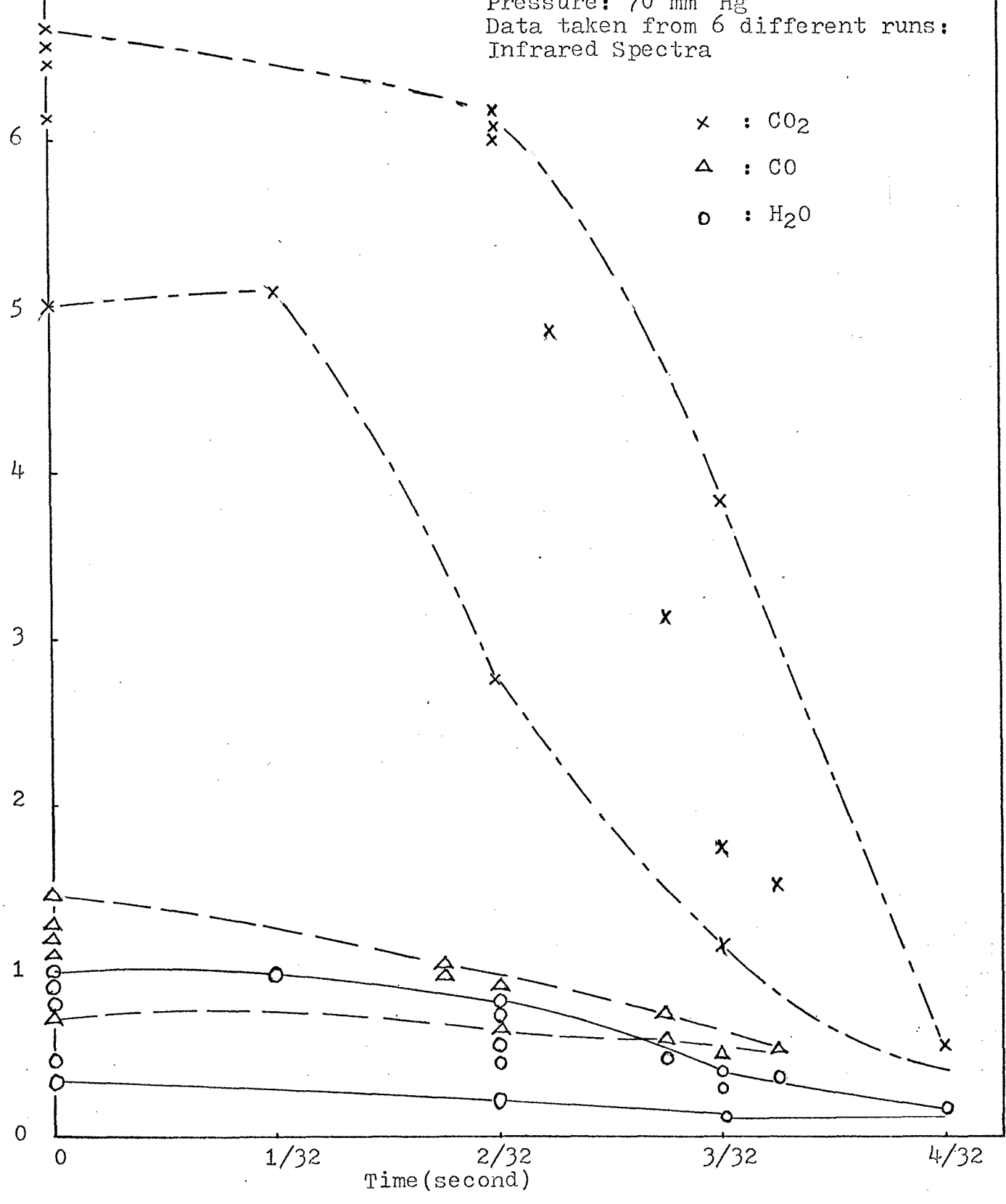


Figure 7 Composition of Flame From IR Spectra During
Quenching of 1:2.5 Butane to O_2 vs Time

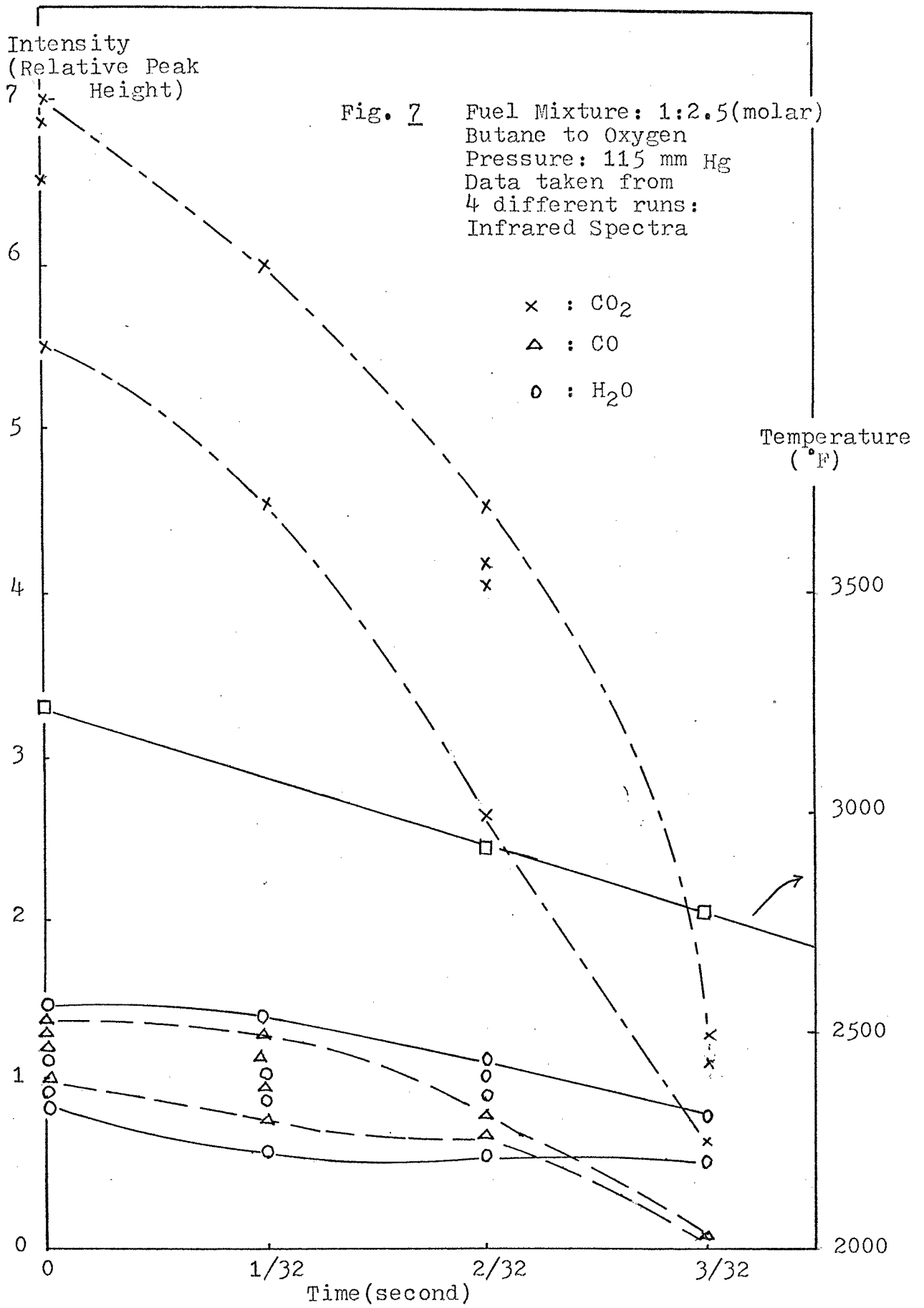


Figure 8 Composition of Flame From UV-Visible Spectra
During Quenching of 1:2.5 Butane to O₂ vs Time

Intensity
(Relative Peak
Height)

Fig. 8

Fuel Mixture: 1:2.5(molar)
Butane to Oxygen
Pressure: 115 mm Hg
UV-Visible Spectra

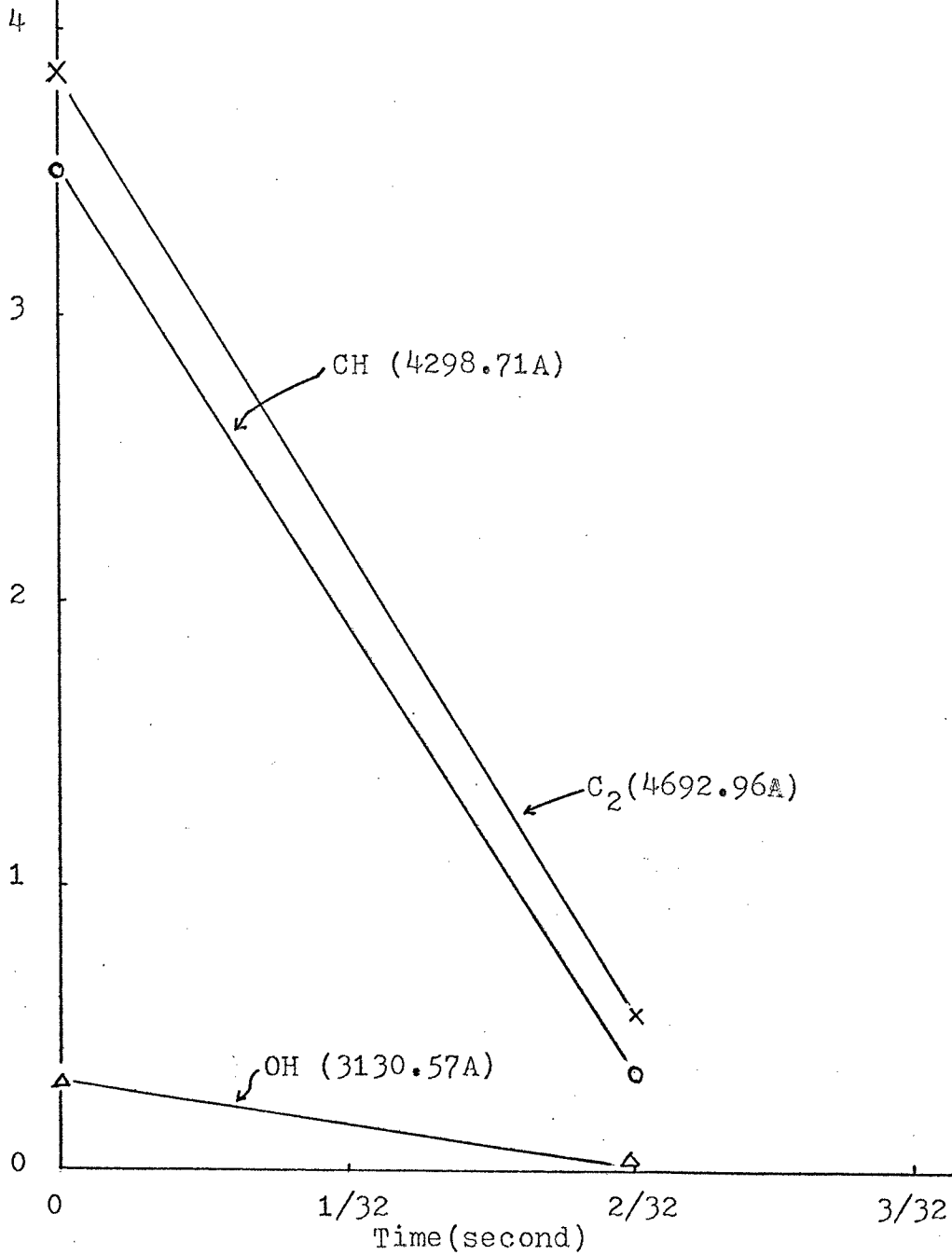
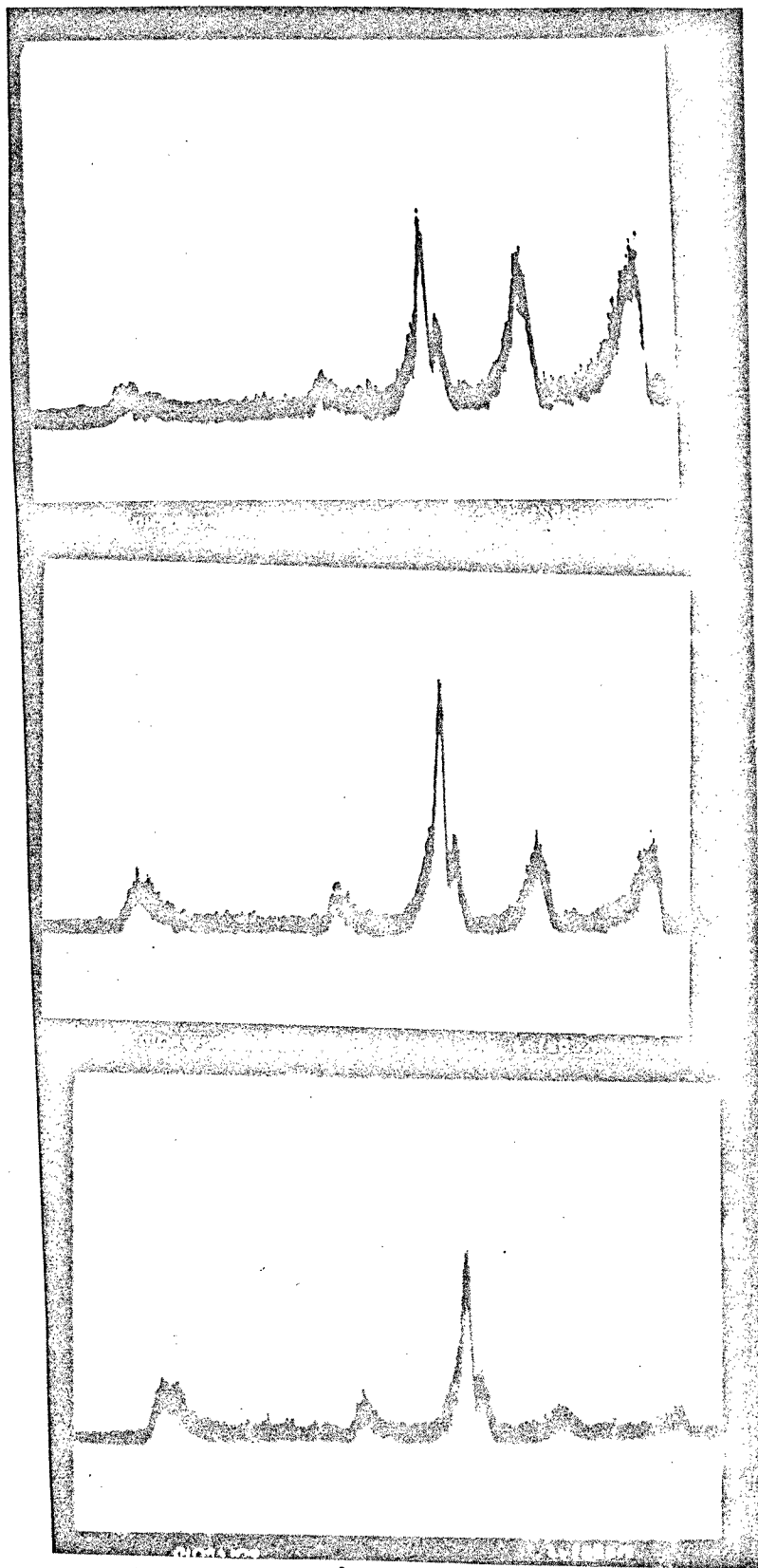


Figure 9 Steady-State UV-Visible Spectra of Methane/
Oxygen Flame in Various Concentrations



No. 1

Methane 22 cc/sec
 Oxygen 24 cc/sec
 O₂/Fuel 1.09
 Pressure 35 mm Hg

No. 2

Methane 22 cc/sec
 Oxygen 29 cc/sec
 O₂/Fuel 1.32
 Pressure 35 mm Hg

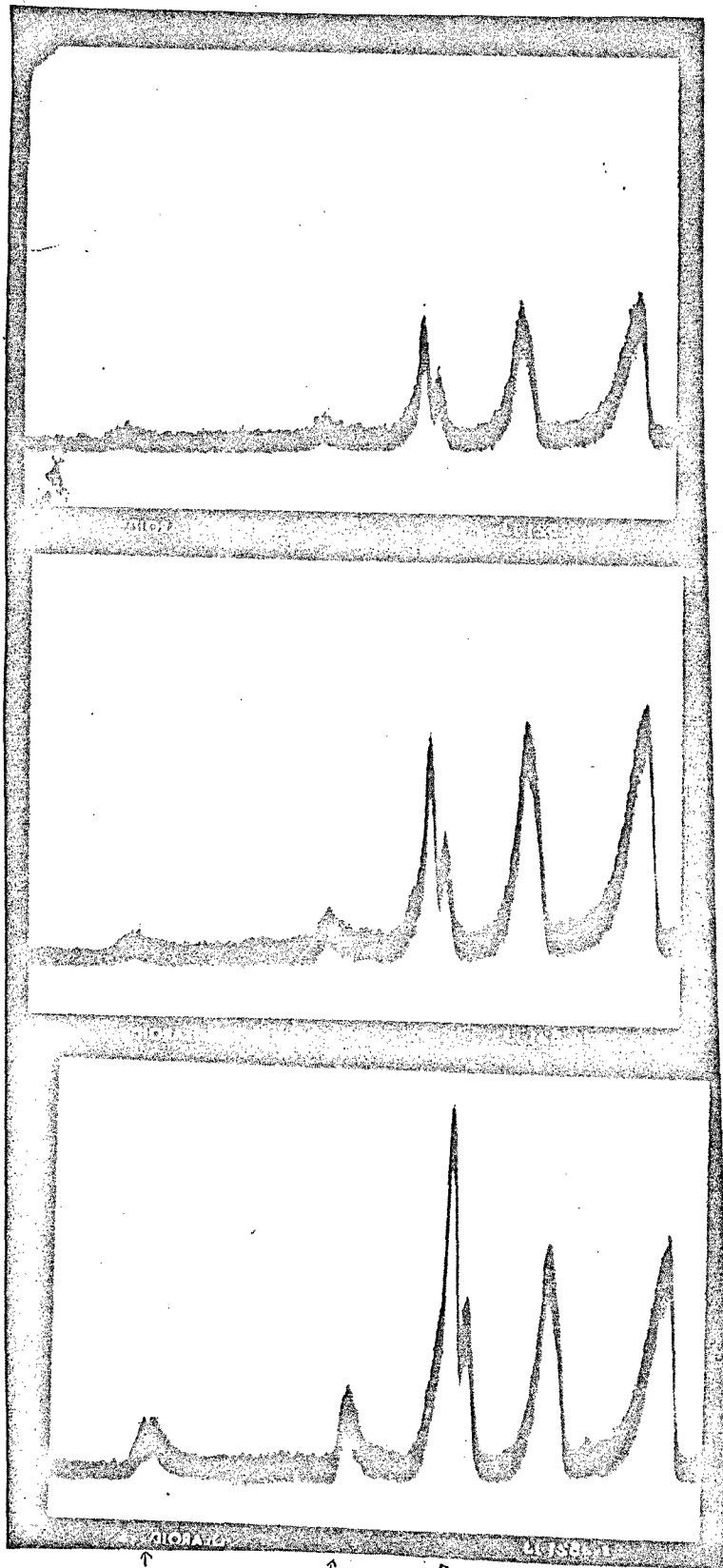
No. 3

Methane 22 cc/sec
 Oxygen 34.5 cc/sec
 O₂/Fuel 1.57
 Pressure 35 mm Hg

↑ OH (3130.57Å)
 ↑ CH (3904Å)
 ↑ CH' (4298.71Å)
 ↘ C₂ (4737Å)
 ↘ C₂ (5165Å)

Fig. 2 Steady-State UV-Visible Spectra of Methane/Oxygen Flame in Various Concentrations

Figure 10 Steady-State UV-Visible Spectra of Butane/
Oxygen Flame in Various Concentrations



No. 1

Butane 8.5 cc/sec
 Oxygen 22.5 cc/sec
 O₂/Fuel 2.65
 Pressure 100 mm Hg

No. 2

Butane 8.5 cc/sec
 Oxygen 28.5 cc/sec
 O₂/Fuel 3.35
 Pressure 100 mm Hg

No. 3

Butane 8.5 cc/sec
 Oxygen 36.5 cc/sec
 O₂/Fuel 4.3
 Pressure 100 mm Hg

\uparrow OH (3130.57Å) \uparrow CH (3904.0Å) \wedge CH (4298.71Å) \leftarrow C₂ (4737.0Å) \leftarrow C₂ (5165.0Å)

Fig. 10 Steady-State UV-Visible Spectra of Butane/Oxygen Flame in Various Concentrations

Figure 11 Steady-State Mass Spectra Data of Non-Sooty
Flame.

Intensity

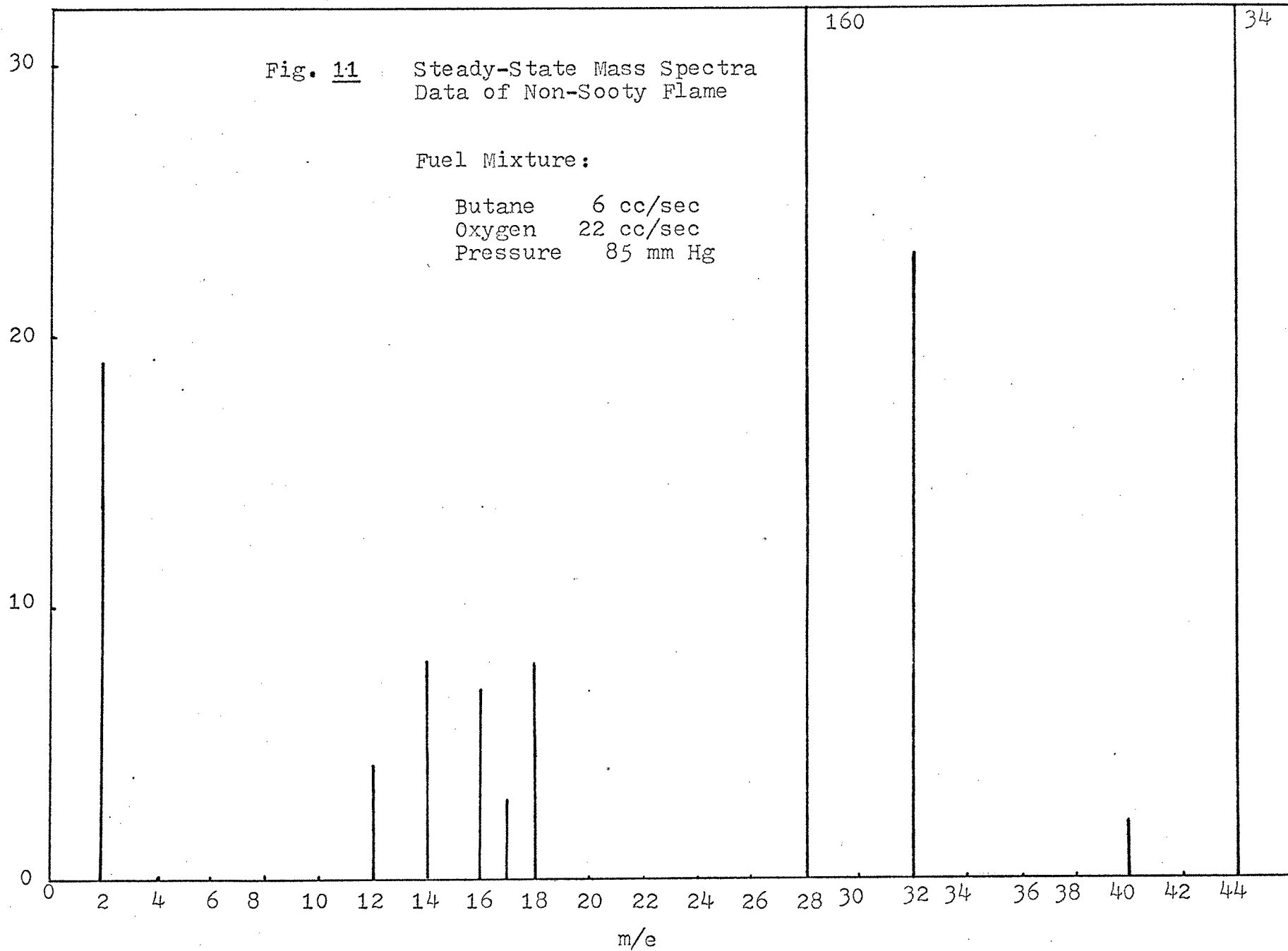


Figure 12 Steady-State Mass Spectra Data of Sooty Flame

Intensity

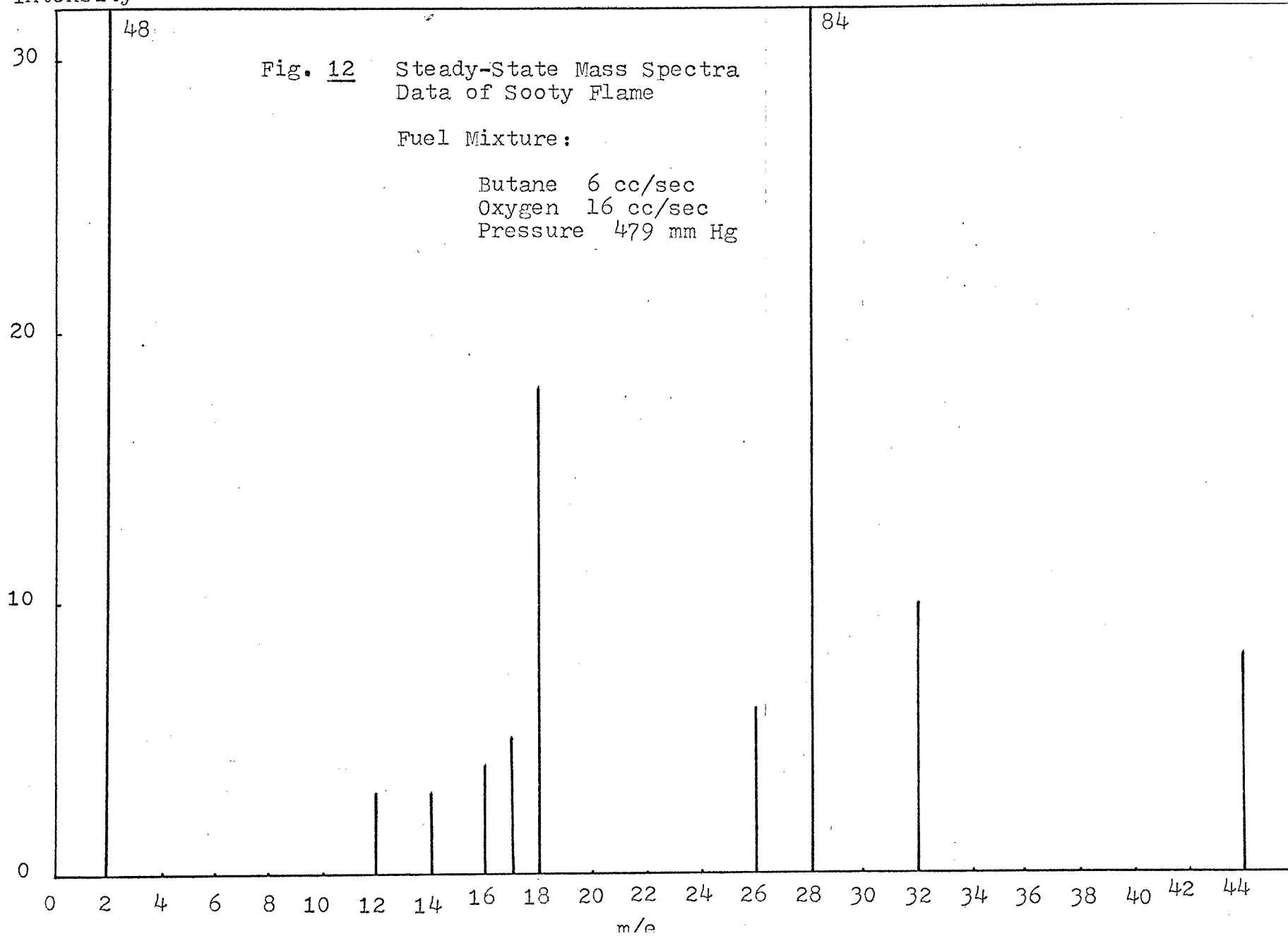
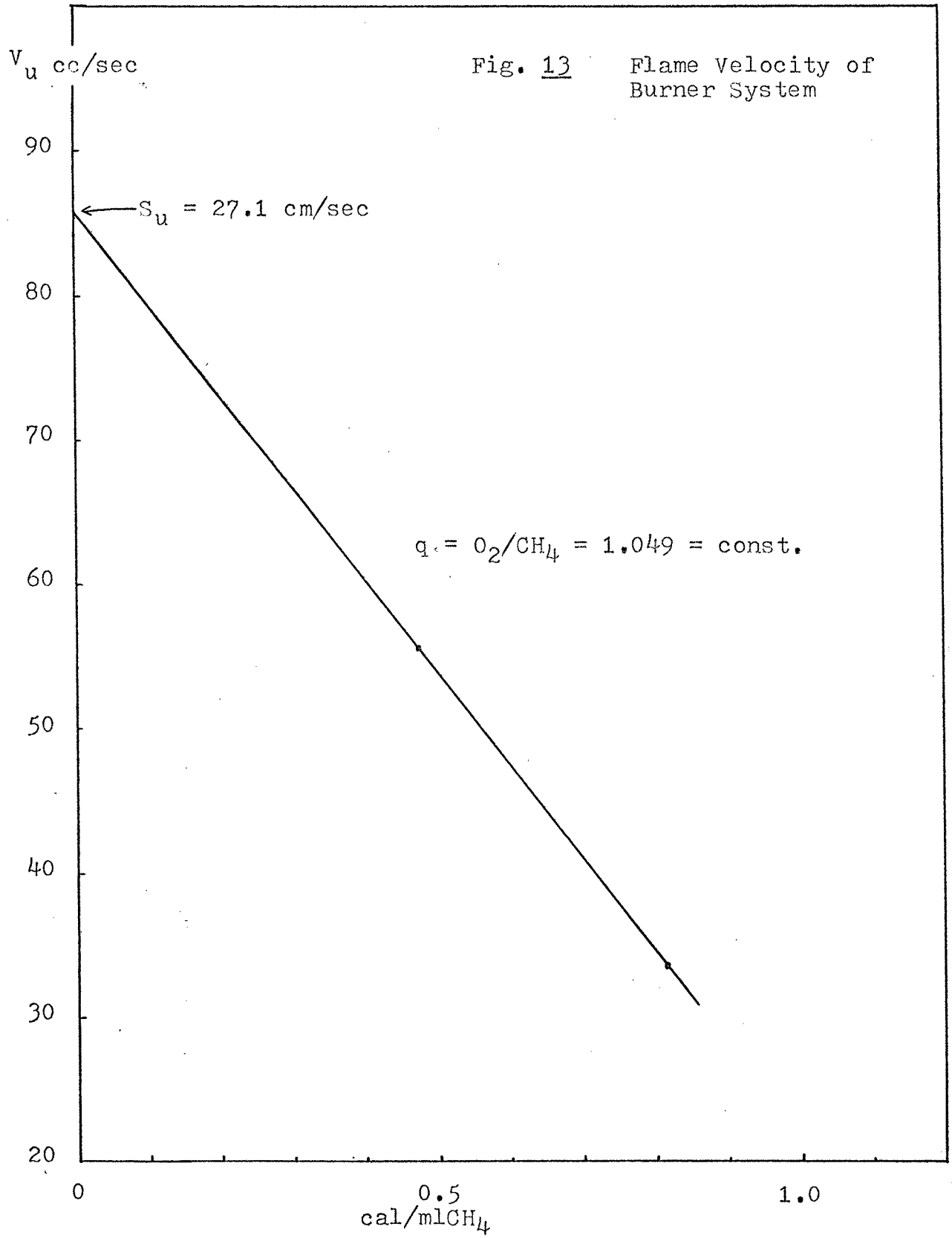


Figure 13 Flame Velocity of Burner System



REFERENCES

1. Levine, R. S., National Aeronautics and Space Administration, Washington, D. C., 1970
2. Homann, K. H., Combustion and Flame, Vol. 11, No. 4 August 1967, pp. 265-287.
3. Mentrop, L., "Experimental and Theoretical Study of Soot Formation and Soot Separation Processes in a Turbulent Diffusion Flame" Rheinisch-Westfalische Lechaische Hochschule, Fakultat fur Nachineweser, Dr. - Ing. Dissertation, 1969.
4. Street, J.C. and Thomas, A., Fuel, 34, 4, (1955)
5. Fenimore, C. P., Jones, G. W., and Moore, G. E., Sixth Symposium (International) on Combustion, Reinhold, 1957, pp. 242-247 .
6. Singer, J. M., Grumer, J., Seventh Symposium (International) on Combustion, Butterworth, 1959, pp. 559-572.
7. Ferguson, R. E., Combust. Flame, 1, 431 (1957)
8. Millikan, R.C., J. Phys. Chem., 66, 794 (1962)
9. Gaydon, A. G. and Wolfhard, H. G., Flames, Chapman and Hall, London, 1960, p.175.
10. Minkoff, G. J. and Tipper C. F. H., Chemistry of Combustion Reactions, Butterworth, 1962.

11. Bonne, U. , Homann, K. H., and Wagner, H. Gg., Tenth Symposium (International) on Combustion, The Combustion Institute (1965), pp. 503-512.
12. Gaydon, A. G., Spectroscopy of Flames, Chapman and Hall, London, (1957)
13. Fristrom, R. M., Flame Structure, McGraw-Hill, New York
14. Bradley, J. N., Flame and Combustion Phenomena, Methuen & Co. Ltd. (1969) p. 116.
15. Homann, K. H. and Wagner, H. Gg., Eleventh Symposium (International) on Combustion, 1966, p. 371.
16. Bent, H. A. and Crawford, Jr., B., J. Phys. Chem., 63, 941 (1959)